Protein resistance driven by polymer nanoarchitecture

Maya K. Endoh[1,*], Yuma Morimitsu[1,2], Daniel Salatto[1], Zhixing Huang[1], Mani Sen[1], Weiyi Li[1], Yizhi Meng[1], David Thanassi[3], Jan-Michael Y. Carrillo[4], Bobby G. Sumpter[4], Daisuke Kawaguchi[5], Keiji Tanaka[2], Tadanori Koga[1,6,*]

[1]Department of Materials Science and Chemical Engineering, Stony Brook University, Stony Brook, New York 11794-2275

[2]Department of Applied Chemistry, Faculty of Engineering, Kyushu University, Fukuoka 819-0395, Japan

[3]Department of Molecular Genetics & Microbiology and Center for Infectious Diseases, Stony Brook University, Stony Brook, New York 11794-5222

[4]Center for Nanophase Materials Sciences and Computational Sciences and Engineering Division, Oak Ridge National Laboratory, Oak Ridge, Tennessee, 37831

[5]Education Center for Global Leaders in Molecular Systems for Devices, Kyushu University, Fukuoka 819-0395, Japan

[6]Department of Chemistry, Stony Brook University, Stony Brook, New York 11794-3400

Abstract

We report that the nanometer-scale architecture of polymer chains plays a crucial role in its protein resistant property over surface chemistry. Protein-repellent (non-charged) a few nanometer-thick polymer layers were designed with homopolymer chains physisorbed on solids. We evaluated the anti-fouling property of the hydrophilic or hydrophobic adsorbed homopolymer chains against bovine serum albumin in water. Molecular dynamics simulations along with sum frequency generation spectroscopy data revealed the self-organized nano-architecture of the adsorbed chains composed of inner nematic-like ordered segments and outer brush-like segments across homopolymer systems with different interactions among a polymer, substrate, and interfacial water. We propose that this structure acts as a dual barrier against protein adsorption.

Fouling is the undesirable accumulation of a material on a wide variety of objects, such as medical devices, ship hulls, and membranes, and has now become a widespread global problem from land to ocean with both economic and environmental penalties[1-4]. Polymers have been used to develop efficient antifouling coatings against protein adsorption from a biological fluid on a solid surface[5-8]. Common chemical characteristics of antifouling polymer surfaces are hydrophilic, electrically neutral, or highly hydrated, as they can strongly bind with water molecules and reduce the interactions with proteins[9-11]. It has been suggested that the "interfacial water molecules" act as a barrier against proteins since a large amount of energy is required to break the strong hydrogen-bonding network[12-14]. Vogler further proposed that protein adsorption does not occur when a contact angle (θ) of a polymer with water is $\theta < 65°$[9].

In addition to this surface chemistry, the structures of polymer surfaces have been shown to play another major role in protein resistance[15]. In this regard, chemically end-grafted polymer chains (i.e., polymer brushes) have been widely utilized[16, 17] since the structure causes the steric repulsion force that prevents protein adsorption[18, 19]. Note that the chemical grafting also helps stabilize polymer coatings under various environmental conditions. With the strategies in mind, poly(ethylene glycol) (PEG) or oligo(ethylene glycol) brushes are well known as the "gold" standard for protein resistance[20-25]. Additionally, polymer brushes composed of zwitterionic molecules[26], hydrophilic polymers[10, 27], and amphiphilic cross-linked polymers[28, 29] as well as self-assembled monolayers[30-33] have been structurally designed to prevent protein adsorption. However, the mechanism of protein anti-fouling at the polymer surface is still controversial.

In this Letter, we show that the nanometer-scale architecture of polymer chains on a solid emerges the protein resistant property against a model protein (bovine serum albumin (BSA)) regardless of a complex interplay of interactions among a polymer, substrate, and interfacial water. The anti-fouling polymer coating designed is composed of non-charged homopolymer chains physically adsorbed onto a solid, resulting in a few

nanometer-thick layer ("polymer nanolayer"). Sum frequency generation spectroscopy (SFG) results clarify (i) the non-significant role of the interfacial water in the emergence of an anti-fouling property and (ii) the two-dimensional chain architecture commonly shared among the polymers in water. Molecular dynamics (MD) simulation results further allow us to establish the generality of the self-organized structures of the polymer nanolayers in water: high-density "loops" (sequences of free segments connecting successive trains) and "tails" (non-adsorbed chain ends)[34] and nematic-like order of "trains" (adsorbed segments) underneath. Hence, we anticipate that the loops/tails act as high-density polydispersed brushes[34] and the trains behave as a molecular level "rigid-wall"[18, 19], such that most of the proteins are not allowed to penetrate into the nanolayer. Our present finding not only provides a better understanding of the mechanism behind protein adsorption on polymer surfaces but also facilitates a versatile design of anti-fouling coatings with common types of synthetic homopolymers regardless of their hydrophilicity.

Polystyrene (PS, weight-average molecular weight (M_w) = 17,000 g/mol, molecular weight distribution (M_w/M_n) =1.05, Pressure Chemical Co., hereafter assigned as PS17k) and poly(2-vinyl pyridine) (P2VP, M_w= 219,000 g/mol, M_w/M_n=1.11, Scientific Polymer Products, Inc.), were used as rational models. The water contact angles of PS was estimated to be 90 ± 1°, while the water contact angle of P2VP was reported to be 67°[35] that is nearly equal to the critical contact angle for protein adsorption defined by Vogler[9]. In addition, polyethylene oxide (PEO, M_n = 20,000 g/mol, Sigma-Aldrich, product no. 83100) was used as a representative of hydrophilic polymers commonly used for protein resistance[36]. To prepare the polymer nanolayers on silicon (Si) substrates, the established solvent rinsing approach[34] was utilized. The detail of the polymer nanolayer preparation including surface treatments of Si has been described elsewhere[35, 37-40] and is also summarized in Supporting Information (SI). We confirmed that the polymer nanolayers composed of the three different polymers covered the substrates homogenously (Figure

S1). The thicknesses of the PS17k, P2VP, and PEO nanolayers used in this study were determined to be 1.9 ± 0.2 nm, 3.0 ± 0.2 nm, 2.5 ± 0.2 nm, respectively, by using X-ray reflectivity. The results are in good agreement with previous reports[35, 37-40]. Based on their thicknesses relative to their radii of polymer gyration in the bulks, the polymer chains in the nanolayer are expected to lie flat on the solid with many solid-segment contacts[37, 38]. We hereafter assign these adsorbed polymer chains as "flattened chains", and the polymer nanolayer consists of the lone flattened chains[37, 38].

Figure 1 shows the optical microscope (OM) images of the nanolayer surfaces after the protein adsorption experiments. Fluorescein isothiocyanate labeled BSA in phosphate buffer saline (PBS) was used for the protein adsorption experiments. The radius of gyration of the BSA in PBS was estimated to be 3.4 nm (Figure S2). The polymer nanolayers were incubated in the protein solution (1 mg/ml) for typically 6 h at 25 °C, then extracted and rinsed with water and thereafter dried with a nitrogen stream. As a control, we also investigated the protein adsorption on a 50 nm-thick P2VP film (Figure 1a) and the bare Si (Figure S4). The OM images revealed a large number of BSA molecules (which appear green on the images) adsorbed on the P2VP thin film and bare Si. On the contrary, as shown in Figure 1b, the OM image demonstrated the anti-fouling property of the P2VP nanolayer. We also found that the PS and PEO nanolayers repel BSA (Figures 1c and 1d). Note that the PEO nanolayer was stable on the substrate for at least 60 days of immersion in the good solvent (i.e., PBS) (Figure S5). The anti-fouling/fouling switching observed in the OM

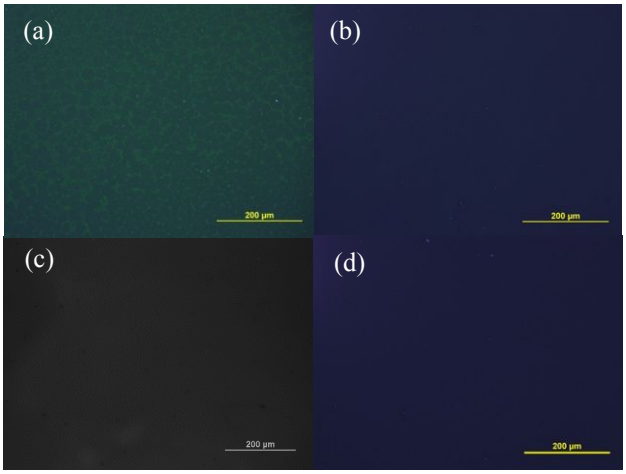

Figure 1. OM images of (a) the 50 nm thick P2VP film, (b) the P2VP nanolayer, (c) the PS17k nanolayer, and (d) the PEO nanolayer after the BSA adsorption experiments. BSA molecules appear green in the images. The scale bars correspond to 200 µm.

results were further confirmed by using a photon counting spectrofluorometer (PC1, Table S1). It is indicative a possible threshold thickness for the switching (Figure S6).

To further extend our claim, two different molecular weights of PS (M_w = 4,000 g/mol, M_w/M_n=1.06 and M_w= 30,000 g/mol, M_w/M_n=1.03, Pressure Chemical Co., hereafter assigned as PS4k and PS 30k, respectively) were also tested. The thicknesses of the PS4k and PS30k nanolayers were 1.9 ± 0.2 nm and the polymer nanolayers covered the substrates homogenously, as previously reported[35, 38, 41]. The PC1 results proved no BSA adsorption on the PS4k and PS30k nanolayers (Table S1 and Figure S6). Hence, we found the emergence of the antifouling property of the polymer nanolayers against the model protein regardless of the degree of polymer hydrophilicity and chain lengths.

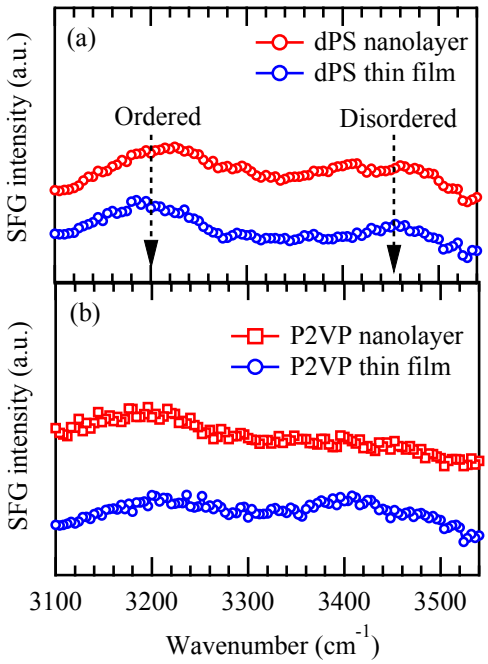

Figure 2. SFG spectra for the dPS nanolayer and dPS thin film (top) and the P2VP nanolayer and thin film in H_2O (bottom) in the O-H vibration region with the *ssp* polarization combination.

We next clarify the role of interfacial water, known as a barrier against protein adsorption[12-14]. For this purpose, SFG measurements were conducted in the O-H vibration region. The details of the SFG experiments are described in SI. Figure 2a shows the SFG spectra for water on the deuterated PS (dPS) thin film (50 nm in thickness) and nanolayer with a *ssp* (SFG/*s*; visible/*s*; and IR/*p*) polarization combination[42]. Note that dPS was used to quantify the vibrational modes of water that overlap with those of hydrogenated PS chains. Two broad peaks were observed at around 3200 and 3450 cm^{-1}. The former can be assigned to the O-H vibrational mode of ordered water molecules which interact with

one another via strong hydrogen bonding[43]. The latter is assignable to the O-H vibrational mode of more disordered water molecules[44] that were previously observed at hydrophilic polymer surfaces[45, 46]. Tanaka and co-workers proposed the population of the disordered water as a gauge of biocompatibility/bioinertness[47]. Interestingly, the SFG data evidences the existence of the ordered and disordered water both on the hydrophobic PS thin film and nanolayer surfaces. The same result is also evidenced for the P2VP nanolayer/water and P2VP thin film/water interfaces (Figure 2b). Although the quantitative comparison of the peak intensity between the two different surfaces is difficult, the SFG data demonstrates that the local water structures are not relevant to the emergence of the present anti-fouling/fouling switching between the nanolayer and thin film. We can also rule out a correlation between the anti-fouling property and the surface roughness of the nanolayers in water (Table S2), which is known as another key parameter for protein adsorption[48].

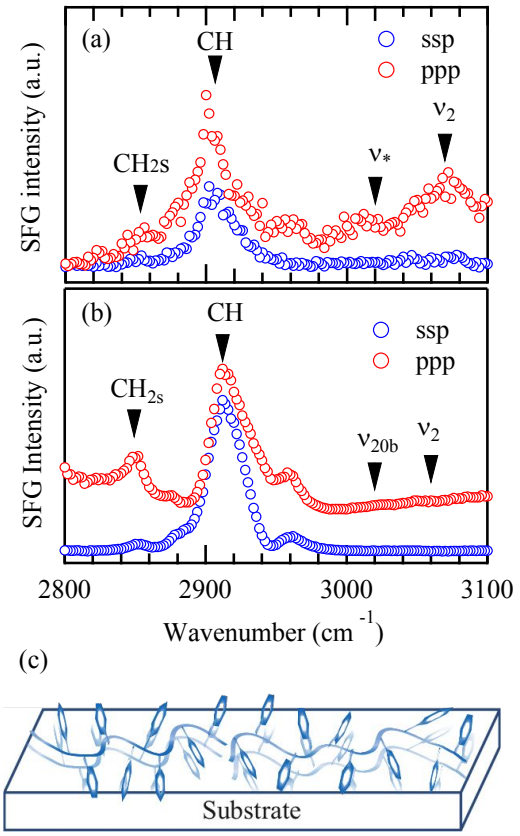

Figure 3. SFG spectra for (a) the P2VP nanolayer and (b) the PS17k nanolayer using the *ssp* and *ppp* polarization combinations in D_2O. The peaks at around 3020 and 3060 cm^{-1} in (b) are attributed to the contributions from the ν_{20b} and ν_2 vibrational modes of phenyl rings (see, Figure S9). (c) Proposed chain conformations of the P2VP and PS17k nanolayers in water.

Grunze and co-workers predicted that the protein adsorption resistance of chemically grafted PEG brushes depended on the chain conformation[18, 49-52]. Their Monte Carlo simulations indicated that a PEG grafted chain on a gold surface, which formed a helical conformation, was inert to protein

adsorption, while a PEG grafted chain on a silver surface, which resulted in a *trans* conformation, did not prevent protein adsorption[50-52]. Motivated by their results, we investigated the chain conformations of the adsorbed chains in water using SFG and explicit solvent coarse-grained MD simulations to understand the origin of the anti-fouling property.

Figure 3 shows the SFG spectra in the C-H stretching vibrational region with the *ssp* and *ppp* combinations acquired at the interface between the P2VP nanolayer and heavy water (D_2O) (panel a). The SFG peaks located at around 2850 cm^{-1} and 2905 cm^{-1} shown in Figure 3a are assigned to symmetric C-H stretching vibration of methylene (CH_2s) group and C-H stretching vibrations of methyne (CH) groups of the backbone chains, respectively[42, 53]. The peak at around 3020 cm^{-1} is attributed to the contributions from inseparable three vibration modes of pyridine rings (see SI, we hereafter assign as the ν^* vibrational mode), while the peak at around 3070 cm^{-1} is attributed to the contribution from the ν_2 vibrational mode[54]. As shown in Figure 3a, the vibrational modes of pyridine rings appear at the *ppp* polarization combination, while those at the *ssp* polarization combination are invisible. This is in contrast to the SFG spectra acquired at the interface between the thin film and water where the vibrational modes with both the *ssp* and *ppp* polarization combinations become very weak (Figure S7), indicating that there is no preferential orientation of the pyridine rings at the water interface. Given the fact that SFG signals with the *ssp* combination are sensitive to the orientation of functional groups along the film normal direction, while those with the *ppp* polarization are sensitive to all directions[42], we conclude that the pyridine rings of the P2VP nanolayer have the tendency to line up along the direction parallel to the film surface in water. In addition, the restriction upon a bond rotation of pyridine groups requires the backbone chains to lie on the substrate[55]. The same conclusion was drawn for the PS17k nanolayer from the SFG results (Figure 3b and Figure S8) and PS thin film (Figure S9).

Consequently, as illustrated in Figure 3c, we propose that both the main chains and the side chains form a two dimensional (2D) structure on the substrate surface in water.

To further generalize the polymer structure in water, we performed explicit solvent coarse-grained MD simulations. The details of the MD simulations (including how to prepare the flattened chains) have been described elsewhere[56, 57] and are also summarized in SI. The interactions between Lennard-Jones (LJ) beads representing water and the flattened chain are either purely repulsive (i.e., hydrophobic) or with a short-range attraction (i.e., hydrophilic) to mimic the experimental conditions. Figure 4 shows representative simulation images of the flattened chains in water. The attractive interaction between the flattened chain and the solid surface was set to 8 k_BT (similar to the PEO-to-Si interfacial energy[40]), while that between the solvent and the solid surface was set to 1 k_BT (similar to water-to-Si interfacial energy). We also changed the persistence lengths (l_p) of polymer chains with $l_p \sim 0$, 2σ, and 4σ (σ is the diameter of a LJ bead)[56] to illuminate the effect of chain rigidity on the resultant chain conformations[58].

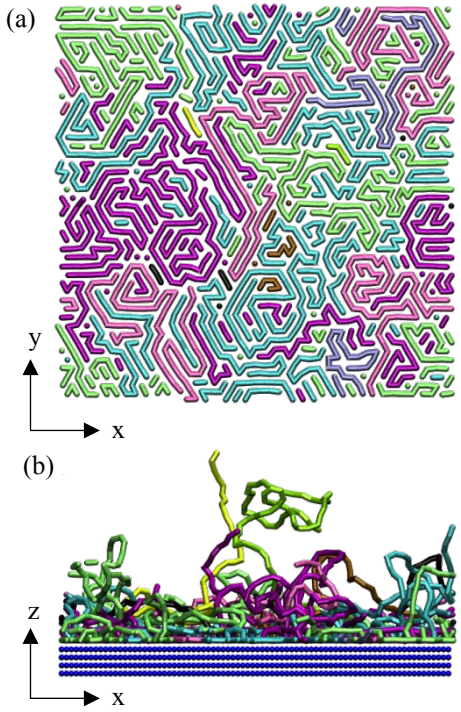

Figure 4. Simulation snapshot of the flattened chains (l_p = 4σ) showing (a) the in-plane structure of the train segments showing nematic-like order of trains and (b) the out-of-plane polydispersed brush conformation of the loops and tails of the flattened chain in a good solvent. The trains are adsorbed beads whose distance is within 1.18 σ from a substrate bead. Each polymer chain is displayed with a different color.

As shown in Figure 4a, the MD results show highly ordered train segments of the flattened chains on the substrate surface in water. Interestingly, the sets of the trains show highly packed nematic-like order[56, 59] in solvents. We also found that the average

neighboring distance between the trains is just about 1σ in both good and poor solvents (Figure S10). Since the polymer model used for the simulations (i.e., linear chains) is general and lacks any specific chemistry, it can fit any polymer and can be mapped back to a real polymer chain based on its Kuhn segment length. Furthermore, we previously reported that the formation of the flattened chains takes place (regardless of the presence of side groups) on weakly interactive solid surfaces as well[37-39]. Therefore, it is reasonable to deduce that the highly-packed 2D chain architecture in water can be generalizable across homopolymer systems with various chemical interactions, chain conformations, and chain rigidity. At the same time, as shown in Figure 4b, the remaining parts of the flattened chains become tails or loops and collectively act as polydispersed brushes[34] with a high "effective" grafting density (the strand-to-strand distance of physisorbed chains was on the order of one statistical Kuhn segment (~1 nm)[56]). According to Sofia and co-workers[60], when open spaces between chemically end-grafted polymer chains become smaller than the effective size of a protein, the protein can no longer adsorb on the end-grafted brush due to the excluded volume effect[61], which is in good agreement with theoretical studies[18, 19, 62]. Hence, the positive structure-property correlation established in this study indicates that the outer high-density tails/loops and the inner densely packed trains, which reduce the amount of available surfaces for the adsorbing protein, act as a "dual" structural barrier.

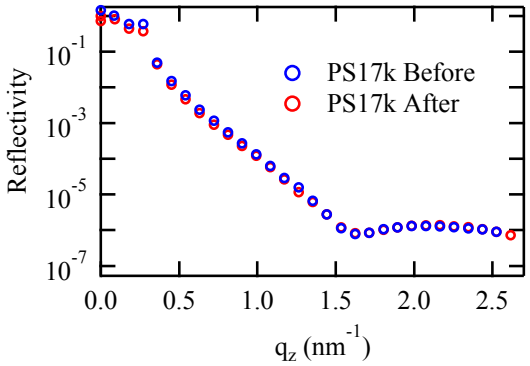

Figure 5. XR profiles of the PS17k nanolayer before and after the PS17k adsorption experiments.

To further test the effectiveness of the flattened chains as an anti-fouling polymer coating, we investigated the adsorption of PS17k onto the PS17k nanolayer. Note that the bulk R_g of PS17k is almost equivalent (3.5 nm) to that of the swollen BSA. The PS17k

nanolayer prepared on the Si substrate was immersed into a bath of a PS17k/toluene solution with the concentration of 1 mg/ml for 5h, then extracted and dried it under ambient conditions. The PS17k nanolayer was then rinsed with chloroform a few times to remove unadsorbed polymer chains and dried at 150 °C for 2h before X-ray reflectivity (XR) experiments. Figure 5 shows the XR profiles in the air before and after the PS17k adsorption experiments. The two XR profiles overlap exactly, proving no changes in the roughness, thickness, and density of the PS17k nanolayer before and after the adsorption experiments. Consequently, this demonstrates the supreme performance of the polymer nanolayer that precludes penetration of chemically identical polymer molecules as well.

In summary, we reveal that the novel architecture of physisorbed (non-charged) homopolymer chains on Si substrates emerges the anti-fouling property against the model protein. The experimental and computational studies elucidated that this nanoarchitecture can be generalized across homopolymers with various chemical interactions, polymer rigidity, and polymer lengths. Our results show one example of the possible anti-fouling behavior of proteins on the polymer surface. As many factors, such as charged groups and hydrophobic patches on a protein and the shape of a native protein conformation (e.g., a globular or rod-like shape), can also come into play[15, 18, 19], subtle differences may be observed for different proteins. However, as theory predicted[18, 19,62], available open spaces between (adsorbed) polymer chains on a substrate is the most critical parameter to prevent protein adsorption. Therefore, the dual chain architecture of the physisorbed polymer chains would prevent adsorption of even very small proteins like cytochrome-c (the size of 3.4 nm[60]).

ACKNOWLEDGMENTS

We thank Ruipeng Li and Masafumi Fukuto for the SAXS and XR experiments and Dmytro Nykypanchuk for the photon counting spectrofluorometer experiments. T.K. and M. E. acknowledge financial support from Kuraray. This research used resources of the Center for Functional Nanomaterials and the National Synchrotron Light Source II, which are U.S. DOE Office of Science Facilities, at Brookhaven National Laboratory under Contract No. DE-SC0012704. The computational/simulations aspect of this work was performed at the Center for Nanophase Materials Sciences, a U.S. Department of Energy Office of Science User Facility. This research also used resources of the Oak Ridge Leadership Computing Facility, which is a DOE Office of Science User Facility supported under Contract DE-AC05-00OR22725.

SUPPORTING INFORMATION. The supporting information contains the details of the sample preparation, experimental techniques, and simulations, small angle X-ray scattering results for BSA, the growth curve of the PS nanolayers, the surface characteristics of the polymer nanolayers, and additional protein adsorption, SFG and simulation results. This material is available free of charge on the ACS Publications website.

Corresponding Authors

***Email:** maya.koga@stonybrook.edu (M.K.E.)

***Email:** tadanori.koga@stonybrook.edu (T.K.)

Notes. The authors declare no competing financial interest.

References

1. Herrwerth, S.; Eck, W.; Reinhardt, S.; Grunze, M. Factors that determine the protein resistance of oligoether self-assembled monolayers-Internal hydrophilicity, terminal hydrophilicity, and lateral packing density, *J. Am. Chem. Soc.* **2003**, 125, 9359-9366.

2. Krishnan, S.; Weinman, C. J.; Ober, C. K. Advances in polymers for anti-biofouling surfaces, *J. Mater. Chem.* **2008**, 18, 3405-3413.

3. Gunari, N.; Brewer, L. H.; Bennett, S. M.; Sokolova, A.; Kraut, N. D.; Finlay, J. A.; Meyer, A. E.; Walker, G. C.; Wendt, D. E.; Callow, M. E. The control of marine biofouling on xerogel surfaces with nanometer-scale topography, *Biofouling* **2011**, 27, 137-149.

4. Yang, W. J.; Cai, T.; Neoh, K.-G.; Kang, E.-T.; Dickinson, G. H.; Teo, S. L.-M.; Rittschof, D. Biomimetic anchors for antifouling and antibacterial polymer brushes on stainless steel, *Langmuir* **2011**, 27, 7065-7076.

5. Dalsin, J. L.; Hu, B.-H.; Lee, B. P.; Messersmith, P. B. Mussel adhesive protein mimetic polymers for the preparation of nonfouling surfaces, *J. Am. Chem. Soc.* **2003**, 125, 4253-4258.

6. Ladd, J.; Zhang, Z.; Chen, S.; Hower, J. C.; Jiang, S. Zwitterionic polymers exhibiting high resistance to nonspecific protein adsorption from human serum and plasma, *Biomacromolecules* **2008**, 9, 1357-1361.

7. Meyers, S. R.; Grinstaff, M. W. Biocompatible and Bioactive Surface Modifications for Prolonged In Vivo Efficacy, *Chem. Rev.* **2011**, 112, 1615-1632.

8. Kyomoto, M.; Moro, T.; Yamane, S.; Hashimoto, M.; Takatori, Y.; Ishihara, K. Poly (ether-etherketone) orthopedic bearing surface modified by self-initiated surface grafting of poly (2-methacryloyloxyethyl phosphorylcholine), *Biomaterials* **2013**, 34, 7829-7839.

9. Vogler, E. A. Structures and reactivity of warer at biomaterial surfaces, *Adv. Colloid Interface Sci.* **1998**, 74, 69-117.

10. Chapman, R. G.; Ostuni, E.; Liang, M. N.; Meluleni, G.; Kim, E.; Yan, L.; Pier, G.; Warren, H. S.; Whitesides, G. M. Polymeric thin films that resist the adsorption of proteins and the adhesion of bacteria, *Langmuir* **2001**, 17, 1225–1233.

11. Ostuni, E.; Chapman, R. G.; Holmlin, R. E.; Takayama, S.; Whitesides, G. M. A survey of structure–property relationships of surfaces that resist the adsorption of protein, *Langmuir* **2001**, 17, 5605–5620.

12. Leung, B. O.; Yang, A.; Wu, S. S. H.; Chou, K. C. The Role of Interfacial Water on Protein Adsorption at Cross-Linked Polyethylene Oxide Interfaces, *Langmuir* **2012**, 28, 5724−5728.

13. Zheng, J.; Li, L.; Tsao, H. K.; Sheng, Y. J.; Chen, S.; Jiang, S. Strong Repulsive Forces Between Protein and Oligo (ethylene glycol) Self-Assembled Monolayers: A Molecular Simulation Study, *Biophys. J.* **2005**, 89, 158−166.

14. Nagasawa, D.; Azuma, T.; Noguchi, H.; Uosaki, K.; Takai, M. Role of Interfacial Water in Protein Adsorption onto Polymer Brushes as Studied by SFG Spectroscopy and QCM, *J. Phys. Chem. C* **2015**, 119, 17193-17201.

15. Roach, P.; Farrar, D.; Perry, C. C. Interpretation of Protein Adsorption: Surface-Induced Conformational Changes, *J. Am. Chem. Soc.* **2005**, 127, 8168-8173.

16. Senaratne, W.; Andruzzi, L.; Ober, C. K. Self-Assembled Monolayers and Polymer Brushes in Biotechnology: Current Applications and Future Perspectives, *Biomacromolecules* **2005**, 6, 2427-2448.

17. Jiang, S.; Cao, Z. Ultralow - Fouling, Functionalizable, and Hydrolyzable Zwitterionic Materials and Their Derivatives for Biological Applications, *Adv. Mater.* **2010**, 22, 920-932.

18. Szleifer, I. Protein Adsorption on Surfaces with Grafted Polymers, *Biophys. J.* **1997**, 72, 595-612.

19. Jeon, S. I.; Lee, J. H.; Andrade, J. D.; de Gennes, P. G. Protein-surface interactions in the presence of polyethylene oxide: I. Simplified theory, *J. Colloid Interface Sci.* **1991**, 142, 149-158.

20. Amiji, M.; Park, K. Surface modification of polymeric biomaterials with poly(ethylene oxide), albumin, and heparin for reduced thrombogenicity, *J. Biomater. Sci. Polym. Ed.* **1993**, 4, 217-234.

21. Prime, K. L.; Whitesides, G. M. Self-assembled organic monolayers – model systems for studying adsorption of proteins at surfaces, , *Science* **1991**, 252, 1164–1167.

22. Bearinger, J. P.; Terrettaz, S.; Michel, R.; Tirelli, N.; Vogel, H.; Textor, M.; Hubbell, J. A. Chemisorbed poly(propylene sulphide)-based copolymers resist biomolecular interactions, *Nat. Mater.* **2003**, 2, 259-264.

23. Elbert, D. L.; Hubbell, J. A. Reduction of fibrous adhesion formation by a copolymer possessing an affinity for anionic surfaces, *J. Biomed. Mater. Res.* **1988**, 42, 55-65.

24. Llanos, G. R.; Sefton, M. V. Does polyethylene oxide possess a low thrombogenicity?, *J. Biomater. Sci., Polym. Ed.* **1993**, 4, 381-400.

25. Xia, N.; May, C. J.; McArthur, S. L.; Castner, D. G. Time-of-flight secondary ion mass spectrometry analysis of conformational changes in adsorbed protein films, *Langmuir* **2002**, 18, 4090-4097.

26. Chen, S.; Zheng, J.; Li, L.; Jiang, S. Strong resistance of phosphorylcholine self-assembled monolayers to protein adsorption: insights into nonfouling properties of zwitterionic materials, *J. Am. Chem. Soc.* **2005**, 127, 14473–14478.

27. Statz, A. R.; Meagher, R. J.; Barron, A. E.; Messersmith, P. B. New peptidomimetic polymers for antifouling surfaces, *J. Am. Chem. Soc.* **2005**, 127, 7972–7973.

28. Xu, J.; Bohnsack, D. A.; Mackay, M. E.; Wooley, K. L. Unusual Mechanical Performance of Amphiphilic Crosslinked Polymer Networks, *J. Am. Chem. Soc.* **2007**, 129, 506-507.

29. Zigmond, J. S.; Letteri, R. A.; Wooley, K. L. Amphiphilic Cross-Linked Liquid Crystalline Fluoropolymer-Poly(ethylene glycol) Coatings for Application in Challenging Conditions: Comparative Study between Different Liquid Crystalline Comonomers and Polymer Architectures, *ACS Appl. Mater. Interfaces* **2016**, 8, 33386-33393.

30. Chapman, R. G.; Ostuni, E.; Takayama, S.; Holmlin, R. E.; L.Yan; Whitesides, G. M. Surveying for Surfaces that Resist the Adsorption of Proteins, *J. Am. Chem. Soc.* **2000**, 122, 8303-8304.

31. Luk, Y.-Y.; Kato, M.; Mrksich, M. Self-assembled monolayers of alkanethiolates presenting mannitol groups are inert to protein adsorption and cell attachment, *Langmuir* **2000**, 16, 9604-9608.

32. Chelmowski, R.; Köster, S. D.; Kerstan, A.; Prekelt, A.; Grunwald, C.; Winkler, T.; Metzler-Nolte, N.; Terfort, A.; Wöll, C. Peptide-based SAMs that resist the adsorption of proteins, *J. Am. Chem. Soc.* **2008**, 130, 14952–14953.

33. Wei, Q.; Becherer, T.; Angioletti-Uberti, S.; Dzubiella, J.; Wischke, C.; Neffe, A. T.; Lendlein, A.; Ballauff, M.; Haag, R. Protein Interactions with Polymer Coatings and Biomaterials, *Angew. Chem. Int. Ed.* **2014**, 53, 8004-8031.

34. Guiselin, O. Irreversible Adsorption of a Concentrated Polymer-Solution, *Europhys. Lett.* **1992**, 17, 225-230.

35. Jiang, N.; Wang, J.; Di, X.; Cheung, J.; Zeng, W.; Endoh, M. K.; Koga, T.; Satija, S. K. Nanoscale adsorbed structures as a robust approach for tailoring polymer film stability *Soft Matter* **2016**, 12, 1801-1809.

36. Campoccia, D.; Montanaroa, L.; Arciola, C. R. A review of the biomaterials technologies for infection-resistant surfaces, *Biomaterials* **2013**, 34, 8533-8554.

37. Gin, P.; Jiang, N. S.; Liang, C.; Taniguchi, T.; Akgun, B.; Satija, S. K.; Endoh, M. K.; Koga, T. Revealed Architectures of Adsorbed Polymer Chains at Solid-Polymer Melt Interfaces, *Phys. Rev. Lett.* **2012**, 109, 265501.

38. Jiang, N.; Shang, J.; Di, X.; Endoh, M. K.; Koga, T. Formation mechanism of high-density, flattened polymer nanolayers adsorbed on planar solids., *Macromolecules* **2014**, 47, 2682-2689.

39. Sen, M.; Jiang, N.; Cheung, J.; Endoh, M. K.; Koga, T.; Kawaguchi, D.; Tanaka, K. Flattening Process of Polymer Chains Irreversibly Adsorbed on a Solid, *ACS Macro Lett.* **2016**, 5, 504-508.

40. Jiang, N.; Sen, M.; Zeng, W.; Chen, Z.; Cheung, J. M.; Morimitsu, Y.; Endoh, M. K.; Koga, T.; Fukuto, M.; Yuan, G.; Satija, S. K.; Carrillo, J.-M. Y.; Sumpter, B. G. Structure-induced switching of interpolymer adhesion at a solid-polymer melt interface *Soft Matter* **2018**, 14, 1108-1119.

41. Y. Morimitsu; D. Salatto; N. Jiang; M. Sen; S. Nishitsuji; B. M. Yavitt; M. K. Endoh; A. Subramanian; C.-Y. Nam; R. Li; M. Fukuto; Y. Zhang; L. Wiegart; A. Fluerasu; K. Tanaka; Koga, T. "Structurally Neutral" Densely Packed Homopolymer-Adsorbed Chains for Directed Self-Assembly of Block Copolymer Thin Films, *Macromolecules* **2019**, 52, 5157-5167.

42. Tsuruta, H.; Fujii, Y.; Kai, N.; Kataoka, H.; Ishizone, T.; Doi, M.; Morita, H.; Tanaka, K. Local Conformation and Relaxation of Polystyrene at Substrate Interface, *Macromolecules* **2012**, 45, 4643-4649.

43. Du, Q.; Freysz, E.; Shen, Y. R. Surface Vibrational Spectroscopic Studies of Hydrogen Bonding and Hydrophobicity, *Science* **1994**, 264, 826−828.

44. Horinouchi, A.; Yamada, N. L.; Tanaka, K. Aggregation States of Polystyrene at Nonsolvent Interfaces, *Langmuir* **2014**, 30, 6565-6570.

45. Morita, S.; Tanaka, M.; Ozaki, Y. Time-Resolved In Situ ATR-IR Observations of the Process of Sorption of Water into a Poly(2-methoxyethyl acrylate) Film, *Langmuir* **2007**, 23, 3750-3761.

46. Noguchi, H.; Hiroshi, M.; Tominaga, T.; Gong, J. P.; Osada, Y.; Uosaki, K. Interfacial Water Structure at Polymer Gel/quartz Interfaces Investigated by Sum Frequency Generation Spectroscopy, *Phys. Chem. Chem. Phys.* **2008**, 10, 4987−4993.

47. Tanaka, M.; Mochizuki, A. Clarification of the Blood Compatibility Mechanism by Controlling the Water Structure at the Blood–Poly(meth)acrylate Interface, *J. Biomater. Sci. Polym. Ed.* **2012**, 21, 1849-1863.

48. Mansouri, J.; Harrisson, S.; Chen, V. Strategies for controlling biofouling in membrane filtration systems: challenges and opportunities *J. Mater. Chem.* **2010**, 20, 4567-4586.

49. Wang, R. L. C.; Kreuzer, H. J.; Grunze, M. Molecular Conformation and Solvation of Oligo(ethylene glycol)-Terminated Self-Assembled Monolayers and Their Resistance to Protein Adsorption, *J. Phys. Chem. B* **1997**, 101, 9767-9773.

50. Harder, P.; Grunze, M.; Dahint, R.; Whitesides, G. M.; Laibinis, P. E. Molecular Conformation in Oligo(ethylene glycol)-Terminated Self-Assembled Monolayers on Gold and Silver Surfaces Determines Their Ability To Resist Protein Adsorption, *J. Phys. Chem. B* **1998**, 102, 426-436.

51. Wang, R. L. C.; Kreuzer, H. J.; Grunze, M. The interaction of oligo(ethylene oxide) with water: a quantum mechanical study *Phys. Chem. Chem. Phys.* **2000**, 2, 3613-3622.

52. Pertsin, A. J.; Grunze, M. Computer Simulation of Water near the Surface of Oligo(ethylene glycol)-Terminated Alkanethiol Self-Assembled Monolayers, *Langmuir* **2000**, 16, 8829-8841.

53. Gautam, K. S.; Schwab, A. D.; Dhinojwala, A.; Zhang, D.; Dougal, S. M.; Yeganeh, M. S. Molecular Structure of Polystyrene at Air/Polymer and Solid/Polymer Interfaces, *Phys. Rev. Lett.* **2000**, 85, 3854−3857.

54. Calchera, A. R.; Curtis, A. D.; Patterson, J. E. Plasma Treatment of Polystyrene Thin Films Affects More Than the Surface, *ACS Appl. Mater. Interfaces* **2012**, 4, 3493-3499.

55. Sen, M.; Jiang, N.; Endoh, M. K.; Koga, T.; Ribbe, A.; Rahman, A.; Kawaguchi, D.; Tanaka, K.; Smilgies, D.-M. Locally favored two-dimensional structures of block copolymer melts on non-neutral surfaces, *Macromolecules* **2018**, 51, 520-528.

56. Carrillo, J. M. Y.; Cheng, S. W.; Kumar, R.; Goswami, M.; Sokolov, A. P.; Sumpter, B. G. Untangling the Effects of Chain Rigidity on the Structure and Dynamics of Strongly Adsorbed Polymer Melts, *Macromolecules* **2015**, 48, 4207-4219.

57. Koga, T.; Barkley, D.; Nagao, M.; Taniguchi, T.; Carrillo, J.-M. Y.; Sumpter, B. G.; Masui, T.; Kishimoto, H.; Koga, M.; Rudick, J. G.; Endoh, M. K. Interphase Structures and Dynamics near Nanofiller Surfaces in Polymer Solutions, *Macromolecules* **2018**, 51, 9462-9479.

58. Rubinstein, M.; Colby, R. H., *Polymer Physics*. Oxford University Press: 2003.

59. Zhang, W.; Gomez, E. D.; Milner, S. T. Surface-Induced Chain Alignment of Semiflexible Polymers, *Macromolecules* **2016**, 49, 963-971.

60. Sofia, S. J.; Premnath, V.; Merrill, E. W. Poly(ethylene oxide) Grafted to Silicon Surfaces: Grafting Density and Protein Adsorption, *Macromolecules* **1998**, 31, 5059-5070.

61. Aubouy, M.; Fredrickson, G. H.; Pincus, P.; Raphaeel, E. End-Tethered Chains in Polymeric Matrixes, *Macromolecules* **1995**, 28, 2979-2981.

62. Satulovsky, J.; Carignano, M. A.; Szleifer, I. KInetic and themodynamic control of protein adsorption, *Proc. Natl. Acad. Sci. USA* **2000**, 97, 9037-9041.

For Table of Contents Use Only

Protein resistance driven by polymer nanoarchitecture

Maya K. Endoh, Yuma Morimitsu, Daniel Salatto, Zhixing Huang, Mani Sen, Weiyi Li, Yizhi Meng, David Thanassi, Jan-Michael Y. Carrillo, Bobby G. Sumpter, Daisuke Kawaguchi, Keiji Tanaka, Tadanori Koga